Single crystal growth, crystal structure and surface characterisation of the binary phase Al45Cr7.

Pascal Boulet, Marie-Cécile de Weerd, Emilie Gaudry, Julian Ledieu, Vincent Fournée

Journal of Physics: Conference Series **1458** (2020) 012016 doi:10.1088/1742-6596/1458/1/012016

Single crystal growth, crystal structure and surface characterisation of the binary phase $Al_{45}Cr_7$

P Boulet[1], **M C de Weerd**[1], **E Gaudry**[1], **J Ledieu**[1], **V Fournée**[1]
[1] Institut Jean Lamour, UMR 7198 Université de Lorraine- CNRS, Nancy, France
Email : vincent.fournee@univ-lorraine.fr

Abstract. A single crystal of the $Al_{45}Cr_7$ crystalline approximant has been grown using the Czochralski method. The structure of this phase has been resolved in the C2/m space group. Chromium atoms are systematically surrounded by Al atoms forming a distorted icosahedron. The icosahedra are linked either by a vertex or a triangular face or overlap along a five-fold axis. The (010) surface of this single crystal has been investigated under ultrahigh vacuum and shows a (1x1) termination at specific bulk planes. The terraces have a nanostructured appearance which is ascribed to the preservation of the $CrAl_{12}$ clusters at the surface. *Ab initio* calculations shows the presence of a deep pseudogap at the Fermi level, due to both a Hume-Rothery effect combined with strong *spd* hybridization. The isoelectronic charge densities highlight the fact that the charges are mainly confined within the $CrAl_{12}$ icosahedron providing support to a certain stability of the clusters which could explain the nanostructured surface morphology encountered. First results on Al thin film deposition on the (010) surface are also reported.

1. Introduction

The Al-Cr binary phase diagram has been investigated by many authors, especially the Al-rich part [1-2]. At least three different phases ($Al_{45}Cr_7$, $Al_{11}Cr_2$ and Al_4Cr) which form peritectically have similar and complex structures, in which atoms are icosahedrally coordinated. They are frequently referred to as "approximant" crystals, in relation with the existence of a metastable icosahedral phase *i*-Al_4Cr [3]. This region of the phase diagram is also of interest for the aluminium industry. It is known that small amounts of Cr added to commercial Al alloys prevent recrystallization and grain growth. Recently [4], the addition of a minute amount of Cr to the Al-20wt% Zn melt has been shown to drastically affect the microstructure through grain refinement. It is suspected that the nucleation of the primary Al phase is assisted through the formation of a transient icosahedral quasicrystals or $Al_{45}Cr_7$ approximant phases in the undercooled liquid at the nanoscale. This assisted nucleation mechanism could explain the high density of grain boundaries observed in twin relationship associated by groups of 5 grains. It could thus be interesting to investigate the interface between such quasicrystal or approximant phase and *fcc* Al. Here we report the successful growth of an $Al_{45}Cr_7$ single crystal, its structure determination, the first results on the (010) surface structure and on Al thin film grown on that surface. The electronic structure of this compound is further studied by density functional theory (DFT) calculations.

2. Experimental and calculation details

2.1. Sample preparation

According to the most recent phase diagram, the $Al_{45}Cr_7$ phase can be obtained through peritectic transformation from an Al-rich solution with nominal composition $Al_{98}Cr_2$ in a temperature window

comprised between 660 and 799 °C [1-2]. An ingot of the desired composition was first prepared by induction melting under an Ar atmosphere. The ingot was then placed in an alumina crucible in a Czochralski furnace, initially evacuated to a pressure of 10^{-6} mbar and back-filled with 1 bar Ar (5.0 grade). An alumina tip was brought into contact with the liquid solution and then pulled at a rate of 0.5 mm/h. Such a slow pulling rate was selected due to the large difference between the composition of the liquid and that of the $Al_{45}Cr_7$ phase. The obtained sample had a distorted rod shape with a diameter of about 8 mm and was about 7 cm long. It consisted in a single crystal in almost the entire volume, but with many Al inclusions. The crystal was oriented by X-ray Laue diffraction and a sample extracted to expose a (010) surface (Fig. 1(a)). Two other small grains with a different orientation were detected at the periphery of the sample, as well as several Al inclusions appearing as black lines and dots on Fig. 1(a). The surface was polished to obtain a mirror appearance. The sample was then mounted on a Ta plate for surface investigations.

2.2. Experimental methods

The single crystal XRD data were collected on a Bruker Kappa Apex II diffractometer equipped with a mirror monochromator and a Mo Kα IμS (λ = 0.71073 Å). The Apex2 program package was used for the cell refinements and data reductions. The structure was solved using direct methods and refined with the SHELXL-2014 programs. Semi-empirical absorption correction (SADABS) was applied to the data. The surface of the single crystal was investigated using a multi-technique ultra-high vacuum (UHV) system equipped with low-energy electron diffraction (LEED) and scanning tunnelling microscopy (STM). Once inserted in the UHV chamber, a clean surface was prepared by cycles of sputtering (Ar+, 1.5 kV, 30 min) and annealing up to 600 °C for 1-2 hours. An optical pyrometer with an emissivity set to 0.35 was used to measure the temperature. Aluminium thin films were deposited using a cold lip source (purity 5N). The deposition rate was set to 0.05 $ML.s^{-1}$.

2.3. Computational details

DFT calculations were performed using the Vienna *ab initio* simulation package (VASP) [5]. The interaction between the valence electrons and the ionic core was described using the projector-augmented wave (PAW) method [6] within the generalized gradient approximation (GGA-PBE) [7], considering the valences for the atoms to be $3s^2\ 3p^1$ (Al), $3p^6\ 3d^5\ 4s^1$(Cr), and using E_{cut} = 450 eV cut-off energy and 224 irreducible k-points. Total energies were minimized until the energy differences become less than 10^{-5} eV between two electronic cycles during the structural optimization. Atomic structure was relaxed till the Hellmann-Feynman forces were as low as 0.02 eV.

3. Results and discussion

3.1. Structure determination

A small crystal was isolated for XRD experiments. The crystallographic data obtained are summarized in Table 1. This compound crystallizes with a centered monoclinic unit cell [8]. The lattice parameters are a = 2.0650(2) nm, b = 0.75978(8) nm, c = 1.0967(1) nm and β = 107.308(2)°, close to those reported He *et al.* [9], the small differences probably being due to small compositional changes. The crystal structure has been successfully refined in the space group C2/m. The positions of all independent atomic position have been found using direct methods, with three independent Cr positions in 2d, 4i and 8j and 16 Al positions (one in 2a, eight in 4i and seven in general position 8j). A series of refinements with the positional and anisotropic thermal parameters converged to the agreement factors R1 = 3.04% and wR2 = 7.28%. All sites have full occupancies as shown in Table 1, and further difference Fourier calculations did not reveal any significant residual electron density peaks. The largest peak in the final difference electron density synthesis was 0.852 $e/Å^3$ and the largest hole was -0.992 $e/Å^3$ with a root mean square (RMS) deviation of 0.192 $e/Å^3$. The positional parameters are listed in Table 2. As shown in Fig. 1(b), all Cr atoms are surrounded by distorted Al icosahedra. The three Cr atomic sites correspond to 3 different polyhedra: red icosahedron (Cr in 2d) are isolated and share only Al atoms with orange

polyhedron, green polyhedron (Cr in 4i) share triangular faces with orange icosahedra and the latest (Cr in 8j) are interpenetrating each other sharing pentagon or triangle faces with other Cr (8j) polyhedron.

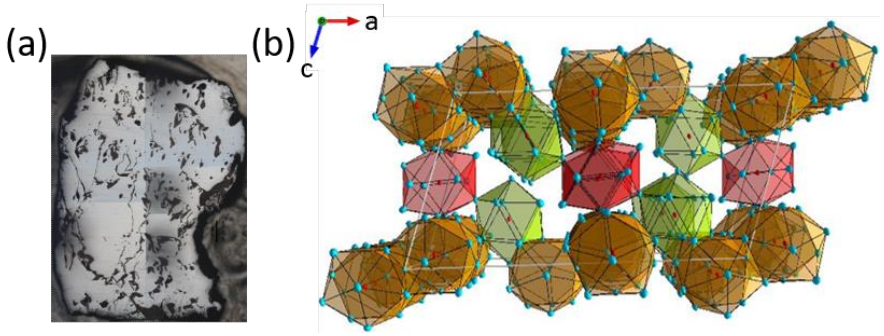

Figure 1: (a) Picture of the (010) oriented sample (~8x5 mm^2). (b) Structure model of the $Al_{45}Cr_7$ phase viewed perpendicularly to the [010] direction and showing the various $CrAl_{12}$ icosahedral polyhedra. Al atoms are in blue, Cr atoms are in red at the centres of the clusters.

Table 1: Crystallographic data, data collection and structure refinement parameters.

Chemical Formulae	$Al_{45}Cr_7$	
Molecular Weight ; Crystal dimensions	1578.10g ; 0.01x0.07x0.07 mm^3	
Wavelength	0.71073 Å	
Space Group	C2/m(12)	
Unit Cell dimensions *(The second column indicates the lattices parameters obtained by VASP)*	a=20.650(2) Å b=7.5978(8) Å c=10.9674(11) Å b=107.308(2)° V = 1642.8(3)Å^3	*a=20.59 Å* *b=7.56 Å* *c=10.92 Å* *b=107.35°* *V = 1622.4 Å^3*
Z	2	
Density / Absorption Coefficient	3.190g/cm^3 / 3.453 mm^{-1}	
Angular Domain	1.95 à 36.93°(0.59 Å resolution)	
	-29<h<29, -12<k<12, -17<l<17	
Reflections observed/Independantes/I>2s	4255/4255/3598	
Rint	0.0808	
Absorption Correction	SADABSV2012/1 multiscan	
Structure solution program	Direct method SHELXL-2014/7(Sheldrick, 2014)	
Goodness of fit on F^2	1.023	
Number of parameters	136	
R1/wR2(observed- I>2s)	0.0304/0.0672	
R1/wR2(all)	0.0407/0.0728	
$\Delta\rho_{max}$, $\Delta\rho_{max}$ ($eÅ^{-3}$)	0.852 et -0.992	

Table 2: Experimental (calculated in italic) atomic coordinates and isotropic displacement parameters.

Atom	Wyckoff position	Occupation factors	x/a	y/b	z/c	Ueq(Å^2)
Cr1	2d	1	0.0	1/2	1/2	0.00387(8)
Cr2	4i	1	0.24950(2) *0.24977*	0.0 *0.0*	0.26200(3) *0.26172*	0.00401(6)
Cr3	8j	1	0.41460(2) *0.41478*	0.32400(3) *0.32534*	0.08170(2) *0.08219*	0.00368(5)
Al1	2a	1	0.0	0.0	0.0	0.00481(14)
Al2	4i	1	0.79320(3) *0.79248*	0.0 *0.0*	0.01190(4) *0.01435*	0.00747(11)
Al3	4i	1	0.59120(3) *0.59041*	0.0 *0.0*	0.34140(4) *0.34233*	0.00905(12)
Al4	4i	1	0.41900(3) *0.41949*	0.0 *0.0*	0.06150(4) *0.06039*	0.00726(11)
Al5	4i	1	0.37150(5) *0.37151*	0.0 *0.0*	0.38750(4) *0.38812*	0.00732(11)
Al6	4i	1	0.27550(4) *0.27595*	0.0 *0.0*	0.50850(4) *0.50957*	0.00681(11)
Al7	4i	1	0.12500(3) *0.12597*	0.0 *0.0*	0.13400(7) *0.13377*	0.00573(11)
Al8	4i	1	0.11520(3) *0.11506*	0.0 *0.0*	0.72990(3) *0.72906*	0.00702(11)
Al9	4i	1	0.02140(3) *0.02185*	0.0 *0.0*	0.25580(5) *0.25598*	0.00703(11)
Al10	8j	1	0.46430(3) *0.46415*	0.18800(6) *0.18835*	0.29560(5) *0.29483*	0.00696(9)
Al11	8j	1	0.31800(3) *0.31843*	0.18500(6) *0.18665*	0.14500(6) *0.14536*	0.00684(8)
Al12	8j	1	0.29350(2) *0.29348*	0.31450(6) *0.31259*	0.36500(5) *0.36565*	0.00823(9)
Al13	8j	1	0.19000(3) *0.18975*	0.31550(6) *0.31459*	0.12050(7) *0.11905*	0.00894(9)
Al14	8j	1	0.16550(2) *0.16546*	0.19300(6) *0.19309*	0.35500(3) *0.35463*	0.00912(9)
Al15	8j	1	0.06920(3) *0.06922*	0.17950(6) *0.18245*	0.48990(5) *0.49006*	0.00857(9)
Al16	8j	1	0.04560(3) *0.04563*	0.30450(6) *0.30324*	0.12170(5) *0.12164*	0.00731(9)

3.2. Surface characterization

The LEED patterns of the (010) surface show sharp spots corresponding to a (1x1) termination (Fig. 2(a)), with a surface unit cell corresponding to a bulk truncation. No significant changes are observed when the annealing temperature is increased from 500 to 600 °C. STM images of the surface show a terrace and step morphology, with a unique step height of 0.38 nm ~ *b*/2. The terraces are relatively small and exhibit frequent holes whose depth is equal to the step height (Fig. 2(d)). Images of individual terraces reveal a nano-clustered surface structure, with a roughness on the order of 0.1 to 0.2 nm. This intrinsic roughness may be due to the existence of $CrAl_{12}$ icosahedra present in the bulk, which may be preserved at the surface. Nevertheless, the fast-Fourier transform of these images still show sharp spots consistent with a surface unit cell parameters $a = 2.1\pm0.1$ nm, $b = 1.0\pm0.1$ nm and $\beta = 107°\pm2°$.

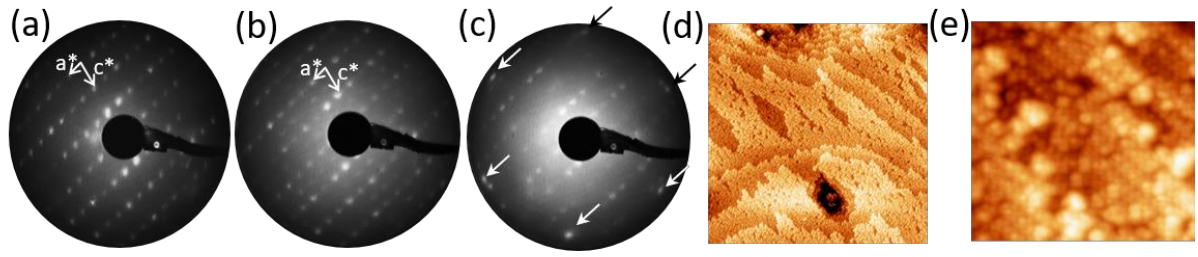

Figure 2: (a) (1x1) LEED pattern of the clean surface (36 eV); (b) c(2x2) pattern obtained after dosing 0.5 ML of Al (36 eV); (c) after dosing 5 ML of Al. Red arrows indicate the Al(111) spots which are nearly in coincidence with some substrates spots. (d) STM image of the clean surface (300x300 nm^2). (e) (25x25 nm^2) is a closer view on the nanostructured surface.

When Al is deposited on this surface at room temperature, it first leads to a c(2x2) surface reconstruction at low coverages (from 0.5 to 1 ML) as observed by LEED (Fig. 2(b)). The surface becomes flatter with atomic rows now becoming clearly visible. With increasing Al coverages (5 to 10 ML), the Al thin film grows with the (111) orientation parallel to the surface plane as evidenced by LEED ([010]$Al_{45}Cr_7$//[111]Al-*fcc*) (Fig. 2(c)). A single rotational domain is deduced from the LEED, corresponding to near-coincidence of the primary Al spots with (4,3), (-3,4), (-8,1), (-4,-3), (8,-1), (3,-4) spots of the $Al_{45}Cr_7$(010) surface.

3.3. Electronic structure

The structural relaxation has been performed based on the experimentally derived structure model. The calculated lattice parameters ($a = 2.059$ nm, $b = 0.756$ nm, $c = 1.092$ nm and $\beta = 107.35°$) and the atomic positions are in good agreement with the experimental ones, with a relative error smaller than 0.5% (Table S2). The partial and total density of states (DOS) are shown in Fig. 3(a). It shows a marked *sp* character in the [-11,-4] eV region, which arises essentially from Al atoms. Cr *d* states lie mostly in the [-3,3] eV region. The partial DOS shows *spd* hybridization in agreement with the shape of the electron density isosurface (Fig. 3b) showing a non uniform charge density distribution between Al and Cr atoms. A marked pseudo-gap is found at the Fermi energy, a feature frequently observed in Al-based quasicrystal and related approximants. The Fermi wave vector can be estimated in a free electron approximation using the values of the valence electron per atom proposed by Mizutani [10]. It leads to $2k_F$=33.46 nm^{-1}, slightly larger than the magnitude of K_{hkl} reciprocal vectors corresponding to the strongest diffraction peaks, taking values between 28 and 30 nm^{-1}. However, there are diffraction peaks with weaker intensities satisfying the Hume-Rothery criterion $2k_F \sim K_{hkl}$. Al and Cr atoms also have small differences in atomic radii and electronegativity (less than 10%), hence the $Al_{45}Cr_7$ system can be assumed to fulfill the Hume-Rothery electronic stabilization criteria. Therefore the origin of the pseudogap is probably due to both a Hume-Rothery mechanism coupled with a strong *spd* hybridization. The strong *spd* hybridization between Al and Cr support the idea of a certain stability associated to the

$CrAl_{12}$ icosahedra surrounding each Cr atoms, which could explain the nanostructured surface morphology encountered.

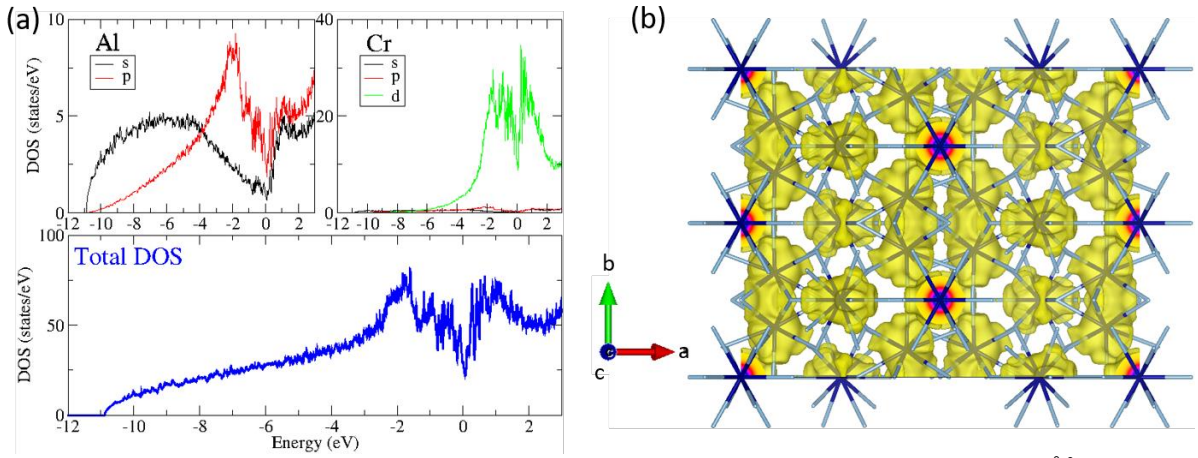

Figure 3: (a) Calculated DOS for the $Al_{45}Cr_7$ compound. (b) Electronic isodensity plotted at 0.037 e/Å^3. The *c* axis is perpendicular to the image plane.

4. Conclusions

We have reported the growth of an $Al_{45}Cr_7$ approximant single grain. The structure has been solved by single crystal XRD. Its (010) surface has been investigated and shows a (1x1) terminated surface at specific bulk planes. The terraces have a nanostructured appearance, ascribed to the preservation of the $CrAl_{12}$ clusters at the surface. DFT calculations show the presence of a deep pseudogap at the Fermi level, due to a Hume-Rothery effect and strong *spd* hybridization. Charge density map indicates a non uniform charge density distribution around Cr atoms. Combined with the *spd* hybridization, it suggests a certain stability of the $CrAl_{12}$ clusters which could explain the nanostructured surface morphology. An Al thin film deposited on the (010) surface leads to the formation of an *fcc* Al film with (111) orientation. Future objectives would be to precisely determine the orientation relationships between the bulk icosahedral clusters and the *fcc* Al grains.

Acknowledgement

We would like to dedicate this article to the memory of our friends Dr. Esther Belin-Ferré and Prof. An-Pang Tsai who recently passed away.

References

[1] Mahdouk K and Gachon J-C 2000 *Journal of Phase Equilibria* **21** 157
[2] Grushko B, Przepiorzynski B and Pavlyuchkov D 2008 *J. Alloys and Comp.* **454** 214
[3] Audier M, Durand-Charre D, Laclau E and Klein H 1995 J. Alloys and Comp. **220** 225
[4] Kurtuldu G, Jarry P and Rappaz M 2013 *Acta Materialia* **61** 7098
[5] Kresse G and Hafner J 1993 *Phys. Rev. B* **47** 558
[6] Kresse G and Joubert D 1999 *Phys. Rev. B* **59** 1758
[7] Perdew J-P, Burke K and Ernzerhof M 1997 *Phys. Rev. Lett.* **78** 1396
[8] Cooper M J 1960 *Acta Cryst.* **13** 257
[9] He ZB, Zou BS and Kuo KH 2006 *Journal of alloys and compounds* **417** L4-L8
[10] Mizutani U and Sato H 2017 *Crystal* **7** 9